Electron Wave Packet Interference in Atomic Inner-Shell Excitation

T. Kaneyasu,[1,3] Y. Hikosaka,[2] M. Fujimoto,[3,4] H. Iwayama,[3,4] and M. Katoh[5,3]
[1]SAGA Light Source, Tosu 841-0005, Japan
[2]Institute of Liberal Arts and Sciences, University of Toyama, Toyama 930-0194, Japan
[3]Institute for Molecular Science, Okazaki 444-8585, Japan
[4]Sokendai (The Graduate University for Advanced Studies), Okazaki 444-8585, Japan
[5]Hiroshima Synchrotron Radiation Center, Hiroshima University, Higashi-Hiroshima 739-0046, Japan

(Received 27 July 2020; accepted 2 February 2021; published 17 March 2021)

We report the observation of quantum interference between electron wave packets launched from the inner-shell 4*d* orbital of the Xe atom. Using pairs of femtosecond radiation wave packets from a synchrotron light source, we obtain time-domain interferograms for the inner-shell excitations. This approach enables the experimental verification and control of the quantum interference between the electron wave packets. Furthermore, the femtosecond Auger decay of the inner-shell excited state is tracked. To the best of our knowledge, this is the first observation of wave packet interference in an atomic inner-shell process, and also the first time-resolved experiment on few-femtosecond Auger decay using a synchrotron light source.

DOI: 10.1103/PhysRevLett.126.113202

The sequential interaction of a pair of time-separated pulses with an atomic or molecular system results in quantum interference between the resulting atomic or molecular wave packets. The advances in laser technology in recent decades have made it possible to produce femtosecond double pulses with precisely controlled waveforms, and to control this quantum interference by appropriately tuning the time delay between the pulses. This method, termed "wave packet interferometry" [1], is now a fundamental tool for studying and manipulating the quantum dynamics of matter. To date, wave packet interferometry has been used in a variety of applications, such as the coherent spectroscopy [2–4] and coherent control [5–7] of atoms, molecules, and condensed matter. Recent advances in these studies benefited by the development of high harmonic generation (HHG) lasers and seeded free-electron lasers (FELs). With the advent of ultrashort extreme ultraviolet (XUV) pulses from HHG, time-domain coherent spectroscopy has become available to probe electron dynamics in the femtosecond to attosecond regime [8,9], and the combination of HHG and frequency comb lasers has enabled precision spectroscopy of atoms in the XUV region, with the aim of testing QED [10,11]. In the meantime, the recent development in seeded FELs has enabled the generation of two phase-locked pulses in the XUV regime [12] and the wave packet interferometry experiment on valence excitation was recently realized with the FERMI FEL [13].

In this Letter, we report the first interference experiment on electron wave packets produced in atomic inner-shell excitation. Inner-shell excitation leads to radiative or nonradiative (Auger) decay which proceeds on a timescale of a few femtoseconds to a few attoseconds. To date, inner-shell excitations in atoms and molecules have been extensively studied using synchrotron light sources [14,15] which provide energy-tunable monochromatized x rays, on a timescale which is quasi-CW compared to the timescale of inner-shell processes. For controlling and probing inner-shell processes on their natural timescale, it is essential to introduce a time-domain approach using ultrashort double pulses with well controlled waveforms. On the other hand, HHG pulses combined with ultrashort IR laser pulses have enabled time-domain access to Auger decay [16] and valence autoionization [17,18] in atoms. However, the use of identical double pulses is simpler and more effective at probing inner-shell processes, as shown in recent theoretical studies [19–21], since this method avoids the complex interpretation necessitated by the IR laser field.

In this work, we use the recently disclosed ability of synchrotron light sources to perform wave packet interferometry experiments [22,23]. Our method is based on the use of the longitudinal coherence between the ultrashort radiation wave packets emitted by individual relativistic electrons passing through undulators placed in series. By using femtosecond XUV radiation wave packets with attosecond-controlled spacing, we observe the time-domain interferogram due to the interference between electron wave packets launched from the inner-shell 4*d* orbital of the Xe atom. The time-domain approach presented here enables us to control the quantum interference in atomic inner-shell processes and to track the femtosecond decay of the short-lived excited state. While the ultrashort property of the radiation wave packets has not been used in our previous studies [22,23], the femtosecond temporal

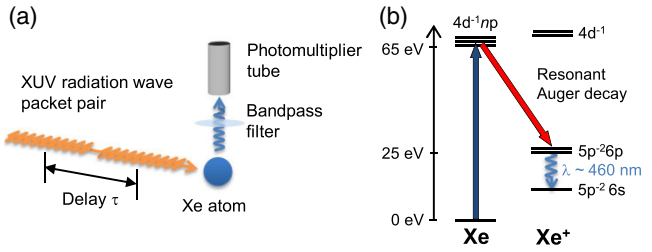

FIG. 1. (a) Experimental scheme for wave packet interferometry in Xe $4d$ inner-shell excitation. The time delay τ between the XUV radiation wave packets is controlled by a phase shifter magnet. The experiment was performed during multibunch operation of the storage ring. The electron beam current was maintained around 10 mA during the measurement. Some 10^9 wave packet pairs were randomly distributed within the 300 ps (FWHM) pulse from the bunch of electrons. Xe gas was provided by an effusive beam from a needle of 0.2-mm inside diameter. (b) Energy level diagram for excitation of the Xe $4d$ electron and its subsequent decays.

duration is essential in this study to track the femtosecond Auger decays of inner-shell excited states. We show that the use of the ultrashort property can overcome the inherent temporal resolution limit in conventional synchrotron experiments.

The main experiment was carried out at beamline BL1U of the UVSOR-III synchrotron [24]. The light source of BL1U consists of twin APPLE-II undulators, which were operated here in the horizontal linear polarization mode. Details of the light source and beamline are given in previous publications [22,23]. Briefly, the number of the magnetic period of the undulator is 10, so that electrons which pass though the undulators emit pairs of 10-cycle radiation wave packets [Fig. 1(a)]. While the waveform of the radiation wave packet was characterized by the 10-cycle oscillation at the fundamental radiation wavelength of around 57 nm, we used the 30-cycle third harmonic component naturally included in the radiation wave packet. To excite the Xe $4d$ electron into the np ($n = 6,7$) orbitals, the peak photon energy of the undulator radiation was adjusted by tuning the pole gap of the undulators. The temporal duration and spectral width of the radiation wave packets were about 2 fs and 3%, respectively. To preserve the waveform of the radiation wave packets, we did not use any optical elements in this experiment. The spatially central part of the undulator radiation was selected by a 0.4-mm-diameter pinhole located 9 m downstream from the center of the two undulators. After passing through the pinhole, the pair of XUV wave packets interacted with Xe atoms. The time delay τ between the radiation wave packets was controlled at the attosecond level by adjusting the electron orbit between the two undulators using a phase shifter magnet. The time delay was calibrated by observing the wave packet interference in the $1snp$ ($n = 5, 6$) excited states of the He atom [25]. Note that the temporal spread of the time delay was limited by the electron beam properties [23]. From the time calibration measurements, we estimated that the temporal spread increased linearly from 10 to 20 as with the increase of time delay from 0 to 20 fs in the present experiment [25].

An energy level diagram of Xe is illustrated in Fig. 1(b). In order to monitor the populations of the $4d^{-1}np$ ($n = 6$, 7) excited states, we detected visible fluorescence photons of 460-nm-wavlength emitted from singly charged ionic states formed via spectator resonant Auger decay [29]. The fluorescence photons were detected by a photomultiplier tube equipped with a bandpass filter, as shown in Fig. 1(a). The detection of visible fluorescence photons allows us to sensitively observe the inner-shell excitation process even with the use of unmonochromatized undulator radiation. By contrast, the detection of ions or total electrons leads a large background resulting from valence photoionization by the whole spectrum of the undulator radiation.

Figure 2(a) shows the fluorescence yield for Xe measured for the two undulators separately, as a function of the gap, in the vicinity of the Xe $4d$ resonances. Both spectra have essentially the same shape, indicating that the waveform shapes of the undulator radiation are almost identical for the two undulators. A broad peak structure resulting from the Xe $4d$ inner-shell resonances appears on a background which mainly originates from valence shakeup ionization by the second and third harmonics leading to the production of $5p^{-2}nl$ excited states [30]. The background gradually increases as the gap increases, which is probably due to the contribution from valence shakeup ionization by the high-energy tail of the fundamental radiation.

To interpret the observed broad peak, a fluorescence yield spectrum measured using monochromatized synchrotron radiation is shown in the inset of Fig. 2(a). Here, the photon energy scale has been roughly adjusted to coincide with the peak photon energy of the undulator radiation, estimated from a spectral measurement of the fundamental radiation (not shown here). This spectrum was recorded at a bending magnet beamline (BL5B), which provides monochromatized synchrotron radiation with a photon energy bandwidth of approximately 0.1 eV. The valence shakeup signal was largely eliminated in this spectrum due to the monochromatization. By comparison with spectroscopic studies on the Xe $4d$ resonances [31,32], the three peaks in the spectrum can be attributed to the $4d_{5/2}^{-1}6p$, $4d_{5/2}^{-1}7p$, and $4d_{3/2}^{-1}6p$ states. These resonance states are not resolved in the unmonochromatized undulator spectra due to the 3% bandwidth of the radiation spectrum.

Using the twin undulators, the visible fluorescence yields were measured as a function of time delay over a range from 0 to 21 fs. Figure 2(b) shows the fluorescence yield for time delays between 0 fs and 5 fs recorded at four different gaps within the resonance peak, together with data recorded at gaps of 60 mm and 63 mm, outside of the resonance peak.

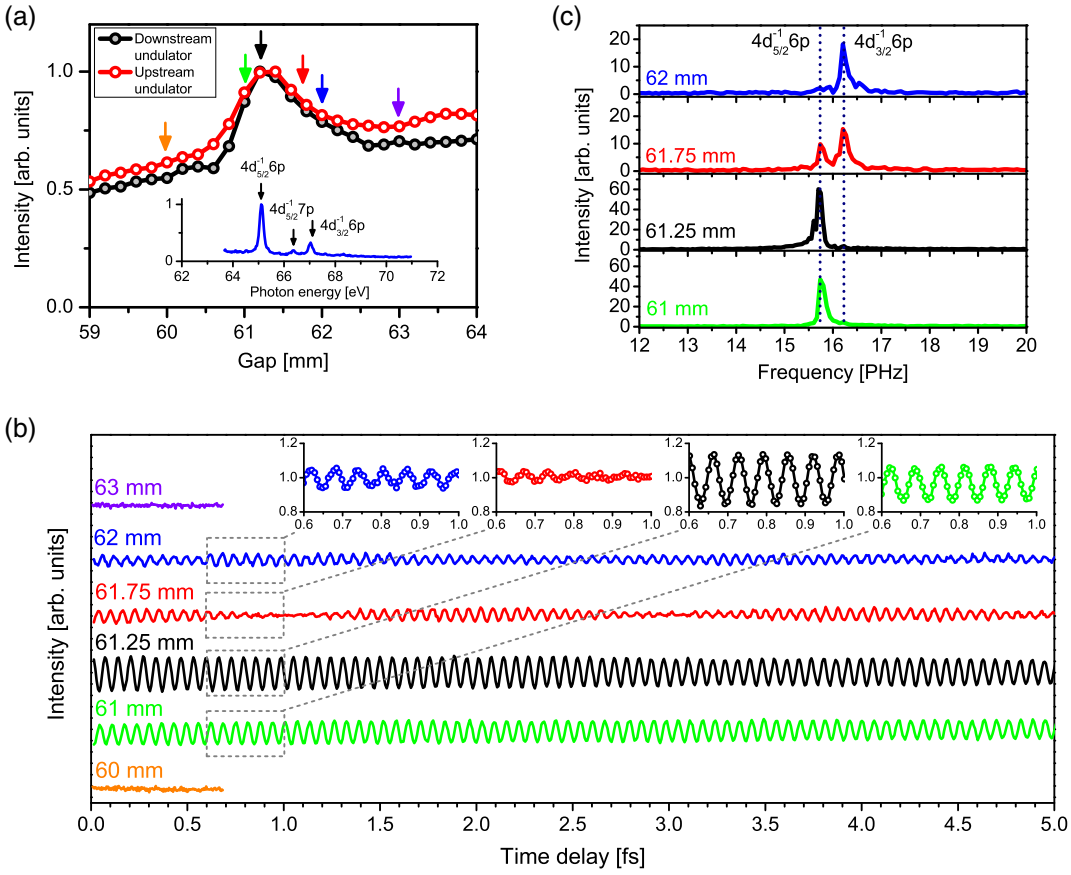

FIG. 2. (a) Fluorescence yield measured as a function of undulator gap for the two undulators operating separately. The inset shows the fluorescence yield spectrum in the region of the Xe $4d$ resonances measured with monochromatized synchrotron radiation. (b) Ramsey fringe spectra for Xe $4d$ excitation (see insets for vertical scales). Fluorescence yields are measured as a function of the time delay at six different gaps. The insets show the expanded sections of the fluorescence yields over the region of 0.6 to 1.0 fs. (c) Fourier transform spectra of the time-domain signals. The Fourier spectra were converted from the time-domain signals using a range of 0 to 15 fs except for the 61.25 mm gap spectrum, where a range of 0 to 21 fs was used. The resonance frequencies from a previous spectroscopic study [31] are indicated by dotted lines.

The corresponding gaps are indicated by arrows in Fig. 2(a). The horizontal axis shows the time delay produced by the phase shifter, to which the minimum achievable time delay of about 2.3 fs must be added to obtain the absolute time delay between the radiation wave packets. The minimum time delay results mainly from the slippage in the upstream undulator, and thus is necessarily longer than the temporal duration of the first radiation wave packet in a pair. The time spectra do not show any modulation at gaps of 60 or 63 mm since the peak photon energy of the undulator radiation here is far detuned from the resonances, and the fluorescence yield is dominated by the valence shakeup ionization process. By contrast, when the undulator gap is tuned within the resonance peak, the time spectra show rapid oscillations, with a period of approximately 60 as. These can be understood as "time-domain Ramsey fringes," which arise from the quantum interference of electron wave packets launched at different times. Here, the oscillation period corresponds to the transition frequency of the Xe $4d^{-1}np$ inner-shell excited states.

The fringe structures in the time spectra exhibit a strong dependence on the undulator gap. While the rapid oscillation dominates the time spectra measured at gaps of 61, 61.25, and 62 mm, this is modulated by a slow beating structure with a period of around 2 fs for a gap of 61.75 mm. In order to interpret these features, we show Fourier transform spectra derived from the time-domain spectra in Fig. 2(c). The peaks observed in the frequency domain correspond precisely to the expected $4d_{5/2}^{-1}6p$ and $4d_{3/2}^{-1}6p$ resonances, [32] within a total uncertainty of 0.04 PHz. The Fourier spectra shown here were derived from the time-domain signals over a range from 0 to 15 fs, except for the spectrum recorded at a gap of 61.25 mm, where we used the full-time delay range [25]. One can see from Fig. 2(c) that at gaps of 61 and 61.25 mm the $4d_{5/2}^{-1}6p$ state is almost exclusively detected. Consequently, the time spectra exhibit a clear sinusoidal modulation which oscillates at the resonant frequency of about 15.7 PHz. From the viewpoint of coherent control, this shows that under these

conditions the excitation probability of the $4d_{5/2}^{-1}6p$ state can be controlled by attosecond-level tuning of the time delay. The beating structure observed in the time spectrum at a gap of 61.75 mm is attributed to the superposition of the $4d_{5/2}^{-1}6p$ and $4d_{3/2}^{-1}6p$ states. The 2-fs period of the beating corresponds exactly to the energy separation between the two states. The weak sinusoidal oscillation in the time spectrum at a gap of 62 mm is due to the excitation of the $4d_{3/2}^{-1}6p$ state. A beat structure may also be superimposed on the sinusoidal oscillation, but it is difficult to discern the small $4d_{5/2}^{-1}6p$ contribution in the time spectrum.

We now discuss the time evolution of the $4d_{5/2}^{-1}6p$ state by using the time spectrum obtained at a gap of 61.25 mm, which corresponds to peak of the undulator radiation close to the energy of the $4d_{5/2}^{-1}6p$ resonance. Figure 3(a) shows this time spectrum for delays ranging from 0 to 21 fs. It is clear that the amplitude of the Ramsey fringes decreases with increasing time delay. This can be explained by considering the time evolution of the first electron wave packet during the sequential interaction. The probability amplitude of the first wave packet decays by a factor of $e^{-\Gamma\tau/2}$, where Γ denotes the decay rate, until the quantum interference occurs when the second wave packet is launched. At long delays, the first wave packet completely decays before the second wave packet is launched and, thus, the interference fringe disappears. According to a theoretical treatment of the decay of excited states [33], the fluorescence yield is expected to be proportional to $1 + e^{-\Gamma\tau/2}\cos\omega\tau$ when fluorescence photons are detected without any time gating. Therefore, we can expect that fringe-contrast decays according to $e^{-\Gamma\tau/2}$ in this experiment. Note that a fringe-contrast decay with the same time constant could be observed even when radiation wave packets of longer durations are used. However, the contrast of the observed fringe amplitude should be reduced in the tracked time range starting from the longer time delay.

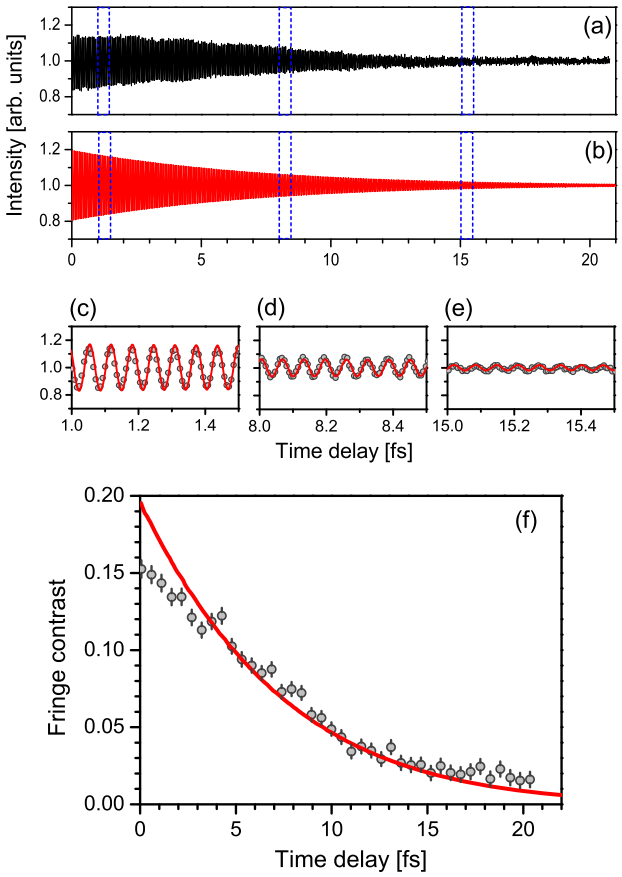

FIG. 3. (a) Fluorescence yield measured at an undulator gap of 61.25 mm. The envelope shows slow beating structures with 2–3 fs period, which is mainly due to the 7-as step in the time delay scan. (b) Calculated time spectrum assuming a 6 fs lifetime for the $4d^{-1}np$ state. (c)–(e) Comparison between the experimental and calculated time spectra in different time delay regions, indicated by dotted blue lines in (a) and (b). (f) Fringe contrast as a function of time delay. The gray circles and red curve show the measurement and calculation results, respectively.

Assuming a 6 fs lifetime for the $4d_{5/2}^{-1}6p$ state [31,34–36], the time-damped Ramsey fringe spectrum can be calculated. Figure 3(b) shows the calculated spectrum, taking into account the temporal resolution of the delay control, and adjusting the transition frequency slightly within the experimental uncertainty in order to reproduce the measurement. In Fig. 3(a) one may observe slow oscillations with a period of ~2 fs, which is not reproduced in Fig. 3(b). These oscillations are artifacts due to the rather large time step (7 as) for measuring the Ramsey fringe of 60-as period. Actual agreements between the spectra in Figs. 3(a) and 3(b) can be judged in the expanded views of the time spectra [Figs. 3(c)–3(e)]. The fringe contrasts in the experiment and calculation are plotted as a function of time delay in Fig. 3(f). The good agreement between experiment and calculation confirms that the reduction in fringe amplitude does indeed arise from the excited state lifetime, proving the time-domain access to femtosecond Auger decay processes.

The present work manifests the capability of synchrotron light sources to probe the time evolution of excited states on timescales of a few femtoseconds. Access to such short timescales has not previously been achieved in time-resolved experiments using synchrotron light sources, since their inherent temporal resolution is limited to a few 10 ps to a few 100 ps by the bunch length of the electrons [37]. Shorter pulses (100 fs) can be generated with the use of special methods to manipulate the bunch length, such as the laser-slicing technique [37] which much reduced photon flux compared with that of usual synchrotron experiments. Even with the methods, femtosecond resolution has been inaccessible. The present study demonstrates that, using the longitudinal coherence between ultrashort radiation wave packets, we can overcome the bunch length limit in synchrotron experiments without reducing the photon flux.

The present study achieved 10-as resolution in the time delay control, with a 2-fs limitation in tracking the decay of short-lifetime states. These experimental limitations can be further improved, respectively, by lowering the electron beam emittance and by reducing the magnetic period number of the undulators. Indeed, a few period undulators can already produce a radiation flux large enough to make the present measurements feasible, provided the electron beam current is increased up to the regular operational condition (300 mA).

In summary, we have observed the interference of electron wave packets created in Xe $4d$ inner-shell excitation using a synchrotron light source. The use of the ultrashort property of the XUV radiation wave packets enabled us to track the few-femtosecond decay of the inner-shell excited states. While the temporal resolution in synchrotron experiments has been thought to be limited by the electron bunch length, the present study clearly shows that processes in much shorter timescale can be accessed by the use of the longitudinal coherence between radiation wave packets. It should be noted that, unlike the two-color coherent control [38,39] and the phase-modulated wave packet interferometry [13] using seeded-FELs, our method can target only single-photon processes. However, the experimental scheme has the potential feasibility to be adopted to even shorter wavelengths, down to the hard x-ray region [23]. Taking advantage of the bright synchrotron light available at short wavelengths, this method will dramatically expand the range of potential targets for ultrafast attosecond science, to the deep inner-shell electrons of a range of elements.

We thank Dr. J. R. Harries (QST) for the critical reading of the manuscript. The experiment was performed at the UVSOR synchrotron facility (Proposal No. 2019-591). This work was supported by the Frontier Photonic Sciences Project of National Institutes of Natural Sciences (Grant No. 01211906) and partly by the JSPS KAKENHI (Grants No. 17H01075, No. 18K03489, No. 18K11945, and No. 20H00164). The construction of BL1U at UVSOR was supported by the Quantum Beam Technology Program of MEXT/JST.

[1] K. Ohmori, Annu. Rev. Phys. Chem. **60**, 487 (2009).
[2] M. J. Snadden, A. S. Bell, E. Riis, and A. I. Ferguson, Opt. Commun. **125**, 70 (1996).
[3] M. Mudrich, F. Stienkemeier, G. Droppelmann, P. Claas, and C. P. Schulz, Phys. Rev. Lett. **100**, 023401 (2008).
[4] L. Bruder, M. Mudrich, and F. Stienkemeier, Phys. Chem. Chem. Phys. **17**, 23877 (2015).
[5] M. A. Bouchene, V. Blanchet, C. Nicole, N. Melikechi, B. Girard, H. Ruppe, S. Rutz, E. Schreiber, and L. Wöste, Eur. Phys. J. D **2**, 131 (1998).
[6] K. Ohmori, Y. Sato, E. E. Nikitin, and S. A. Rice, Phys. Rev. Lett. **91**, 243003 (2003).
[7] K. L. Litvinenko *et al.*, Nat. Commun. **6**, 6549 (2015).
[8] P. Tzallas, E. Skantzakis, L. A. A. Nikolopoulos, G. D. Tsakiris, and D. Charalambidis, Nat. Phys. **7**, 781 (2011).
[9] T. Okino, Y. Furukawa, Y. Nabekawa, S. Miyabe, A. A. Eilanlou, E. J. Takahashi, K. Yamanouchi, and K. Midorikawa, Sci. Adv. **1**, e1500356 (2015).
[10] D. Z. Kandula, C. Gohle, T. J. Pinkert, W. Ubachs, and K. S. E. Eikema, Phys. Rev. A **84**, 062512 (2011).
[11] L. S. Dreissen, C. Roth, E. L. Gründeman, J. J. Krauth, M. Favier, and K. S. E. Eikema, Phys. Rev. Lett. **123**, 143001 (2019).
[12] D. Gauthier, P. R. Ribič, G. De Ninno, E. Allaria, P. Cinquegrana, M. B. Danailov, A. Demidovich, E. Ferrari, and L. Giannessi, Phys. Rev. Lett. **116**, 024801 (2016).
[13] A. Wituschek *et al.*, Nat. Commun. **11**, 883 (2020).
[14] *VUV, and Soft X-Ray Photoionization*, edited by U. Becker and D. A. Shirley (Plenum Press, New York, 1996); and references therein.
[15] K. Ueda, J. Phys. B **36**, R1 (2003).
[16] M. Drescher, M. Hentchel, R. Kienberger, M. Uiberacker, V. Yakovlev, A. Scrinzi, Th. Westerwalbesloh, U. Kleineberg, U. Heinzmann, and F. Krausz, Nature (London) **419**, 803 (2002).
[17] S. Gilbertson, M. Chini, X. Feng, S. Khan, Y. Wu, and Z. Chang, Phys. Rev. Lett. **105**, 263003 (2010).
[18] B. Bernhardt, A. R. Beck, X. Li, E. R. Warrick, M. J. Bell, D. J. Haxton, C. W. McCurdy, D. M. Neumark, and S. R. Leone, Phys. Rev. A **89**, 023408 (2014).
[19] C. Buth and K. J. Schafer, Phys. Rev. A **91**, 023419 (2015).
[20] S. Chatterjee and T. Nakajima, Phys. Rev. A **94**, 023417 (2016).
[21] S. Chatterjee and T. Nakajima, Phys. Rev. A **96**, 063406 (2017).
[22] Y. Hikosaka, T. Kaneyasu, M. Fujimoto, H. Iwayama, and M. Katoh, Nat. Commun. **10**, 4988 (2019).
[23] T. Kaneyasu, Y. Hikosaka, M. Fujimoto, H. Iwayama, and M. Katoh, Phys. Rev. Lett. **123**, 233401 (2019).
[24] M. Adachi, H. Zen, T. Konomi, J. Yamazaki, K. Hayashi, and M. Katoh, J. Phys. Conf. Ser. **425**, 042013 (2013).
[25] See Supplemental Material at http://link.aps.org/supplemental/10.1103/PhysRevLett.126.113202 for details about the time delay calibration, estimation of the temporal spread of time delay, and Ramsey fringe spectra in the full-time delay range, which includes Refs. [26–28].
[26] NIST Atomic Spectra Database (ver. 5.6), http://physics.nist.gov/asd.
[27] P. Elleaume, J. Phys. Colloques **44**, 333 (1983).
[28] K. Je Kim, Nucl. Instrum. Methods **219**, 425 (1984).
[29] M. Meyer, A. Marquette, A. N. Grum-Grzhimailo, U. Kleiman, and B. Lohmann, Phys. Rev. A **64**, 022703 (2001).
[30] S. Alitalo, A. Kivimaki, T. Matila, K. Vaarala, H. Aksela, and S. Aksela, J. Electron Spectrosc. Relat. Phenom. **114–116**, 141 (2001).
[31] D. L. Ederer and M. Manalis, J. Opt. Soc. Am. **65**, 634 (1975).
[32] P. A. Heimann *et al.*, J. Phys. B **20**, 5005 (1987).
[33] M. M. Salour, Rev. Mod. Phys. **50**, 667 (1978).

[34] G. C. King, M. Tronc, F. H. Read, and R. C. Bradford, J. Phys. B **10**, 2479 (1977).
[35] S. Masui, E. Shigemasa, A. Yagishita, and I. A. Sellin, J. Phys. B **28**, 4529 (1995).
[36] O.-P. Sairanen, A. Kivimäki, E. Nõmmiste, H. Aksela, and, S. Aksela, Phys. Rev. A **54**, 2834 (1996).
[37] R. Schoenlein, T. Elsaesser, K. Holldack, Z. Huang, H. Kapteyn, M. Murnane, and M. Woerner, Phil. Trans. R. Soc. A **377**, 20180384 (2019).
[38] K. C. Prince *et al.*, Nat. Photonics **10**, 176 (2016).
[39] D. Iablonskyi *et al.*, Phys. Rev. Lett. **119**, 073203 (2017).